

Fracture analysis and mapping of the Cretaceous Boquillas Formation, Black Gap Wildlife Management Area, Brewster County, TX

Williams, J.W., Alsleben, H., and Enderlin, M.B.

School of Geology, Energy, and the Environment, Texas Christian University, Fort Worth, TX 76129



Abstract

The Eagle Ford Shale in south Texas is one of the most prolific unconventional hydrocarbon plays in the world (Breyer, 2016). In 2015, natural gas and oil from this field hit peak production numbers at 5,539 MMcf (million cubic feet) and 1,118,648 Bbl (barrels) per day, respectively (Texas RRC, 2016). In September of 2016, the Eagle Ford shale produced 1,027,000 Bbl per day, approximately 23% of unconventional oil produced in the United States for that month (EIA, 2016). In order for this low-permeability formation to produce, companies are using hydraulic fracturing, a stimulation treatment used in low-permeability rock whereby fluids are pumped at high pressures into reservoirs, causing new fractures to open and/or the reactivation of existing fractures (Schlumberger, 2016).

The aim of this study is to identify any geomechanical and geochemical properties that optimize fracture connectivity within the Boquillas Formation, the West Texas Eagle Ford Shale equivalent. The Boquillas Formation is composed of alternating beds of calcareous shale, marl and limestone, rock types defined by their calcite, clay, and silica content.

Here we present a geologic map completed at 1:6000 scale of the area in and around Heath Canyon as well as data taken from four outcrop stations within Heath Canyon. Mapping was completed to understand local deformation. Fracture spacing, frequency, and vertical persistence measurements were taken in the field as well as rock strength and hardness measurements. Rock strength was measured using the Equotip Bambino 2 (Fig. 1) and rock hardness was determined using a point load penetrometer (dimpler) (Fig. 2). Energy-dispersive x-ray fluorescence (ED-XRF) data determined the bulk elemental composition of the material and semi-quantitatively assess chemical variations throughout the outcrop. ED-XRF analyses were completed using a Bruker Tracer III-V spectrometer (Fig. 3). ED-XRF and strength/hardness data from this study suggests that fracture frequency and length are affected by the clay and calcium carbonate content, and, by inference, the strength of the rock.



Figure 1: Equotip Bambino 2 micro-rebound hammer metal hardness tester (Image from Proceq).

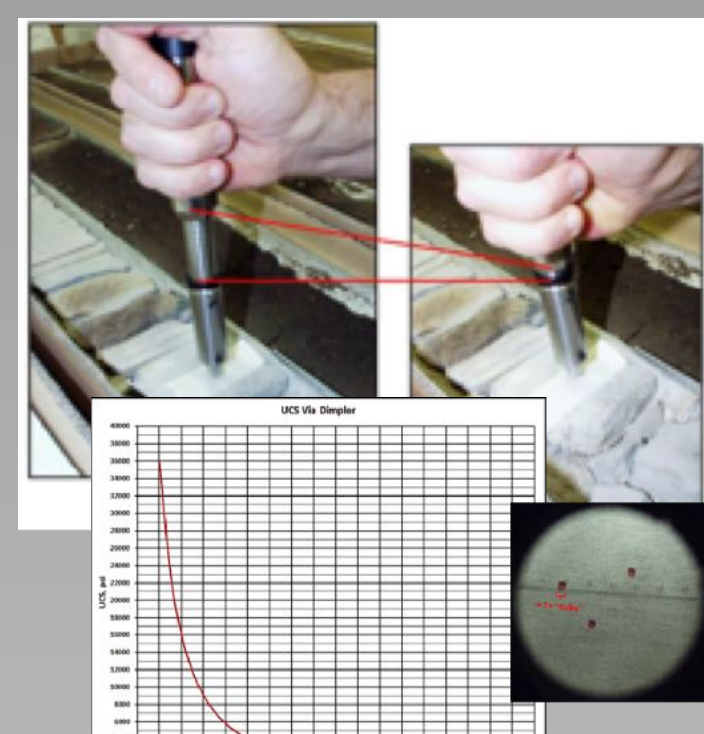


Figure 2: Point load penetrometer (dimpler) mode of operation (top) and graph showing the relationship between 'tick' marks and unconfined compressive strength.



Figure 3: Bruker Tracer III-V energy-dispersive x-ray fluorescence (ED-XRF) spectrometer (Image from Bruker 2015).

Background

Black Gap Wildlife Management Area (WMA) encompasses approximately 103,000 acres (160 mi²) (414 km²) within the Trans-Pecos region of west Texas (Fig. 1). The Trans-Pecos is bounded by the Pecos River to the east, the thirty-second parallel to the north, and by the Rio Grande River to the south and west. The wildlife management area is east of Big Bend National Park. Black Gap WMA is a part of the Chihuahuan desert biome and is under the management of Texas Parks and Wildlife.

The Trans-Pecos region of Texas has experienced multiple major deformational episodes including: (1) Late Paleozoic shortening associated with the Ouachita orogeny, (2) Cretaceous to Tertiary Laramide shortening and transpressional deformation, and (3) Tertiary Basin and Range extension (Muehlberger and Dickerson, 1989; Maxwell et al., 1967; St. John, 1966) (Fig. 5). The Trans-Pecos also experienced widespread magmatism from the Mesozoic through the Cenozoic related to the Laramide orogeny and Basin and Range extension (Turner et al., 2011).

The rock units within Black Gap WMA are Cretaceous or younger. The Late Cretaceous marine rocks were deposited on carbonate platforms northeast of the Chihuahuan Trough, which formed during late Triassic rifting associated with the opening of the Gulf of Mexico (Fig. 6). This rift basin was located east-northeast of a subduction related magmatic arc, which was the source for Late Cretaceous clastic sediments in the Trans-Pecos (Lehman and Busbey, 2007). The carbonate platforms that developed in the Early Cretaceous were the site of deposition for the Santa Elena Limestone, the Buda Limestone, and the Boquillas Formation, which are the dominant units in the study area (Fig. 7).

Aside from being widespread in the study area, rocks that make-up the Coahuila Platform underlie the majority of the Trans-Pecos region (Lehman and Busbey, 2007).

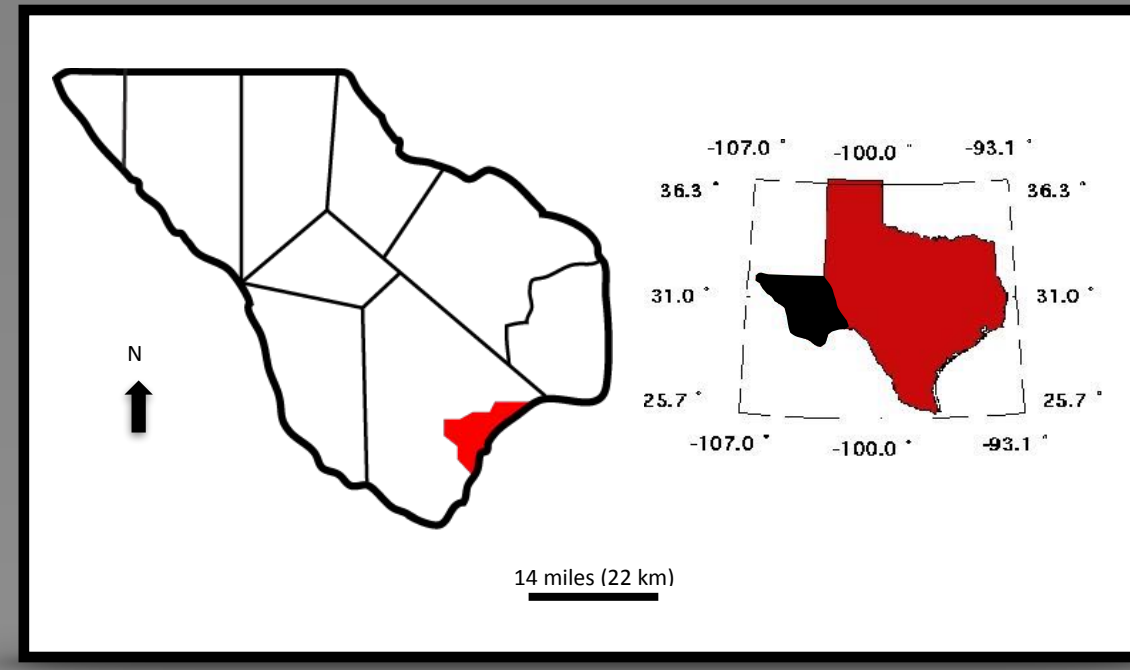


Figure 4: Locations of the Trans-Pecos region of Texas (right, black polygon) and Black Gap Wildlife Management Area (left, red polygon).

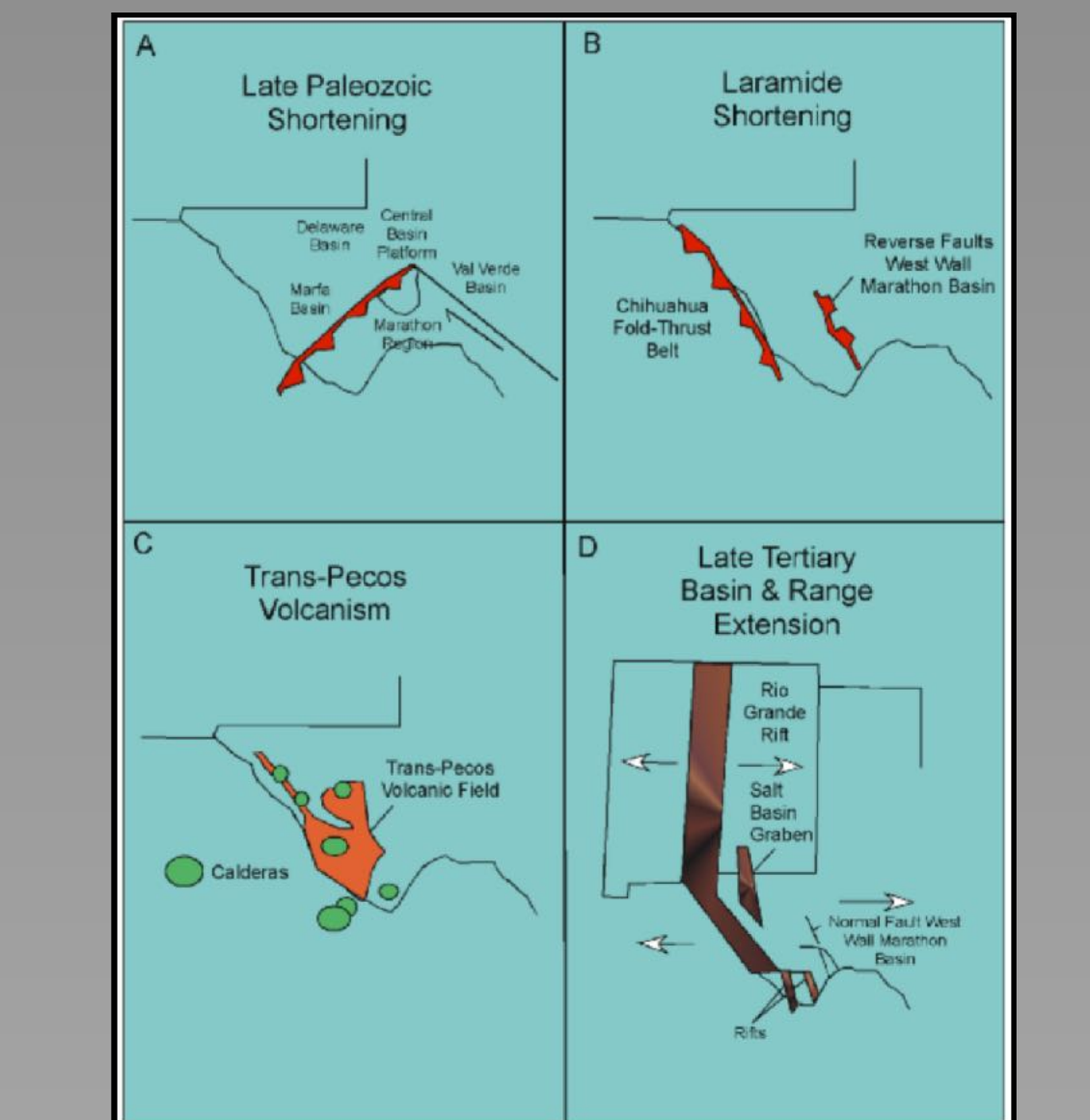


Figure 5: Major tectonic episodes within Trans-Pecos Texas (from Muehlberger and Dickerson, 1989).

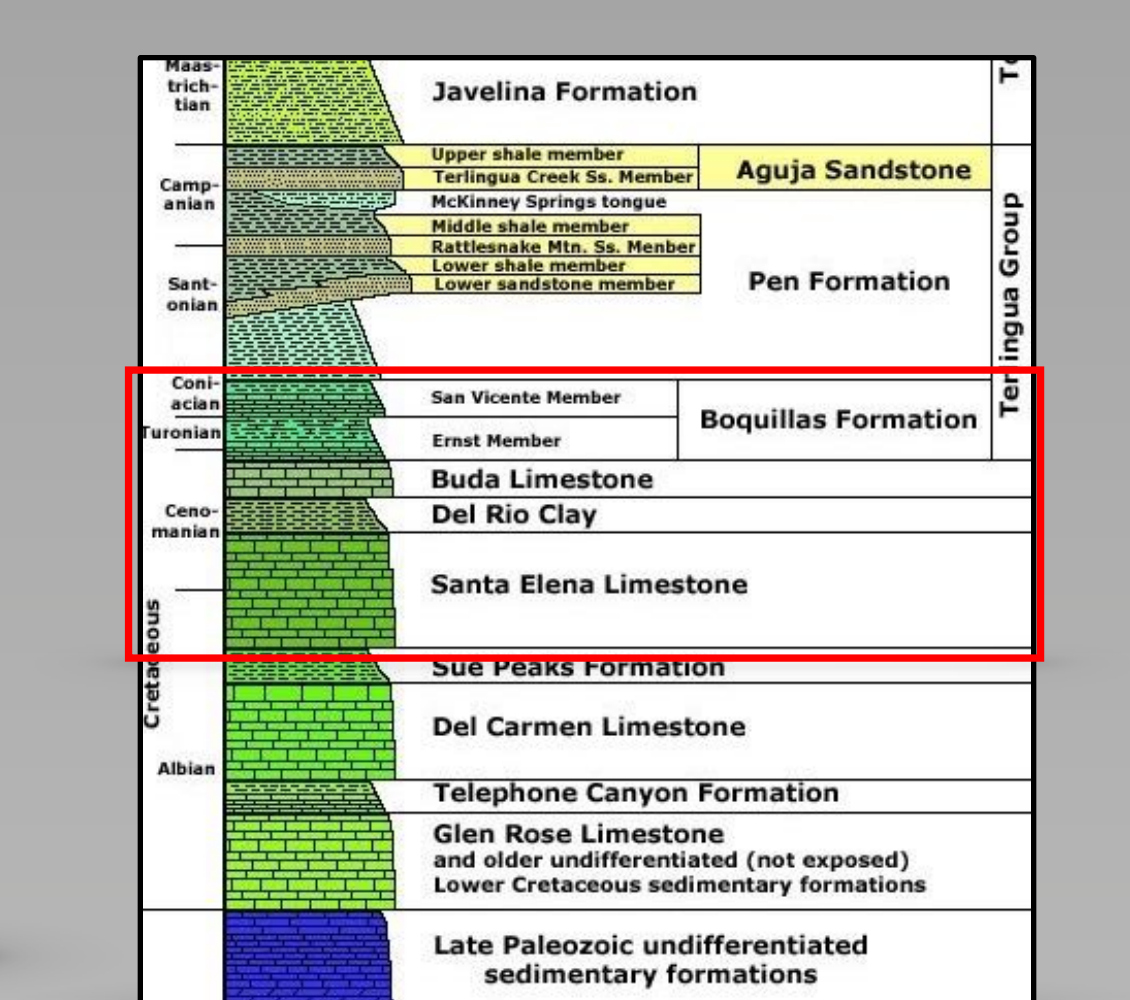


Figure 6: Paleogeographic reconstruction of the North American continent during the deposition of the Boquillas Formation (82.2 Ma). The black oval outlines the approximate location of the Chihuahuan Trough (left) and the carbonate platform on which sediments were deposited during this time (modified from Blakey, 2017).

Figure 7: Stratigraphic Column of the Big Bend area (Modified from Tiedemann, 2010).

Data

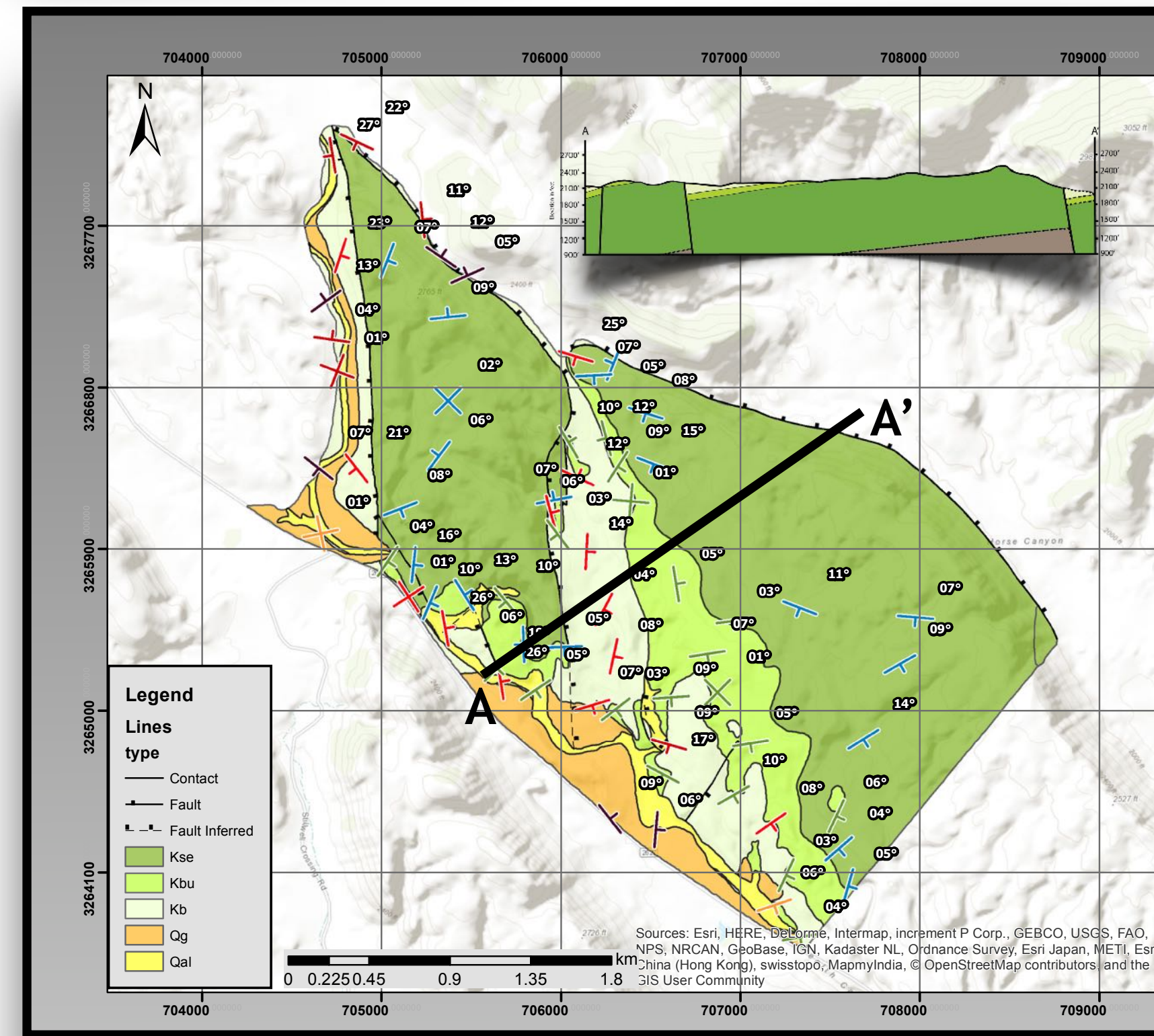


Figure 8: (left) Geologic map (1:6000) of the area in and around Heath Canyon, Black Gap Wildlife Management Area.

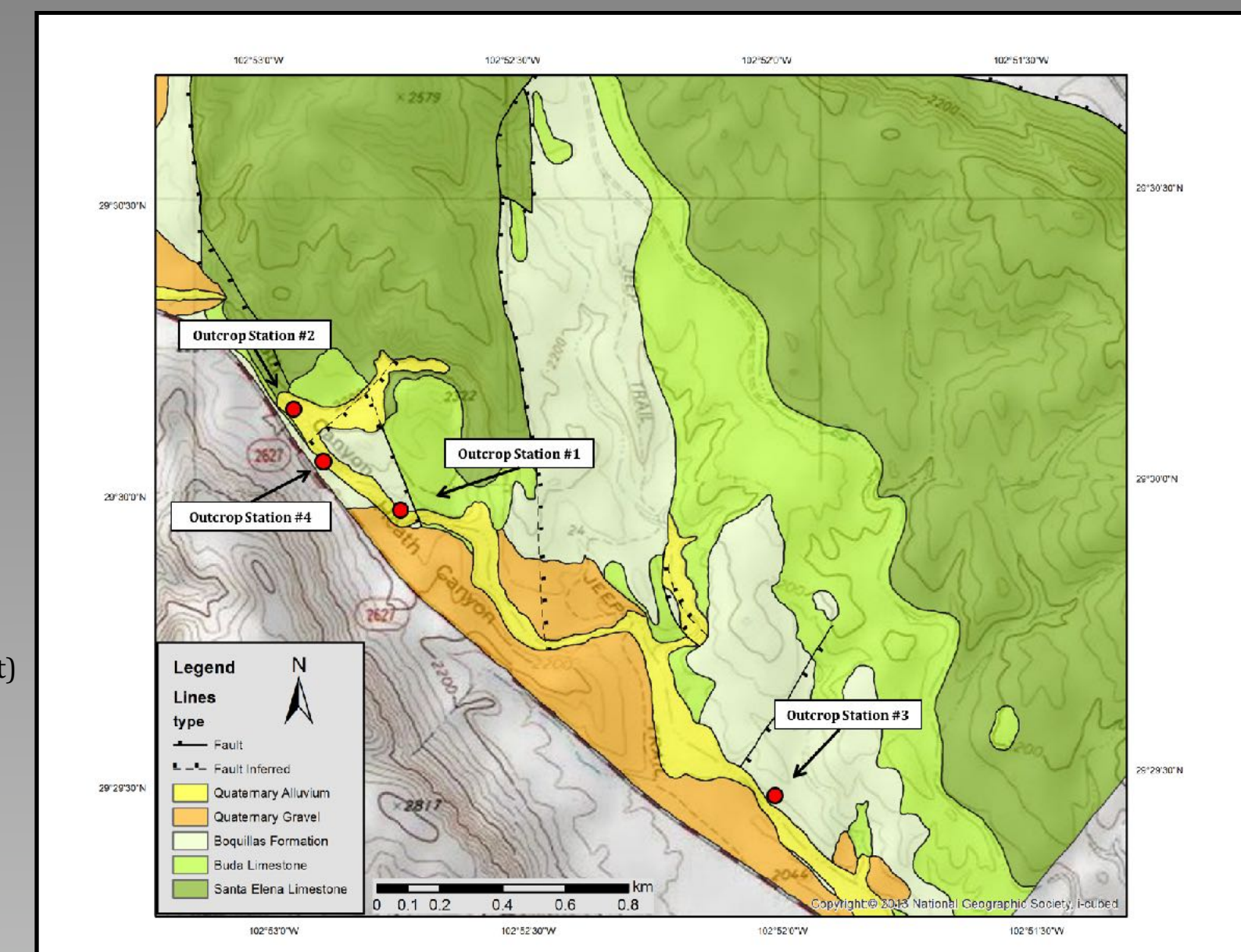


Figure 9: (right) Location of the four outcrop stations within Heath Canyon.

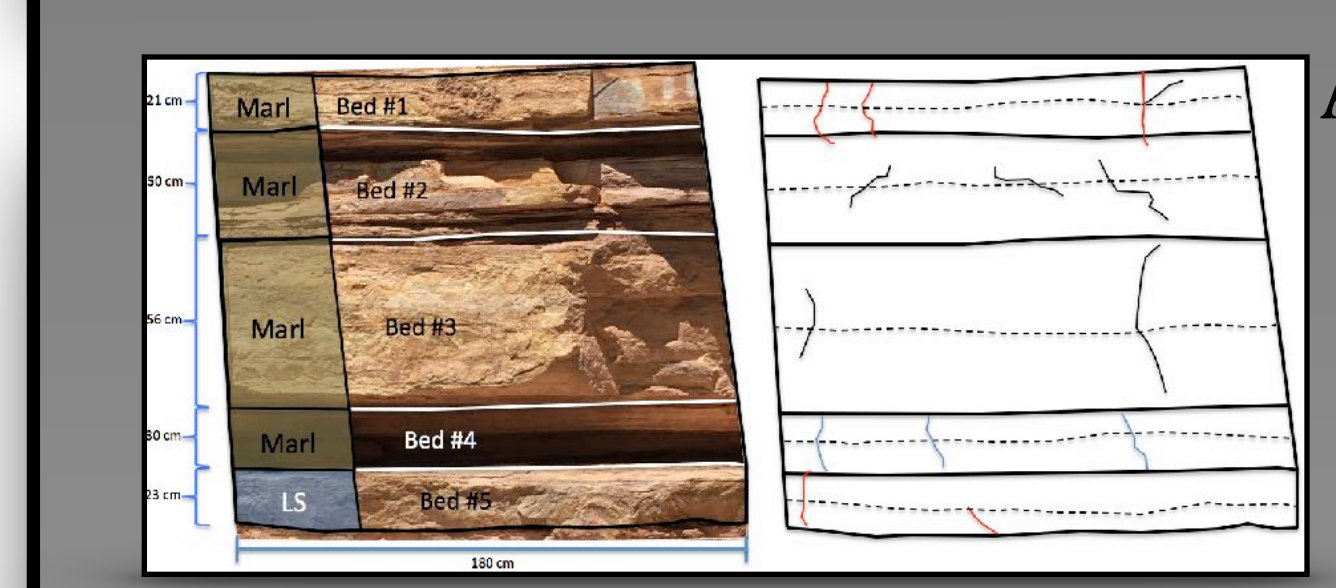


Figure 10 A-D: Outcrop stations 1-4 (A-D) respectively photos and line drawings with associated data tables below (photos do not have the resolution to include all fractures in line drawings).

Table 1: Summary of Fracture Data for Station 1. Columns include Fracture ID, Orientation, Length, Frequency, etc.

Table 2: Summary of Fracture Data for Station 2. Columns include Fracture ID, Orientation, Length, Frequency, etc.

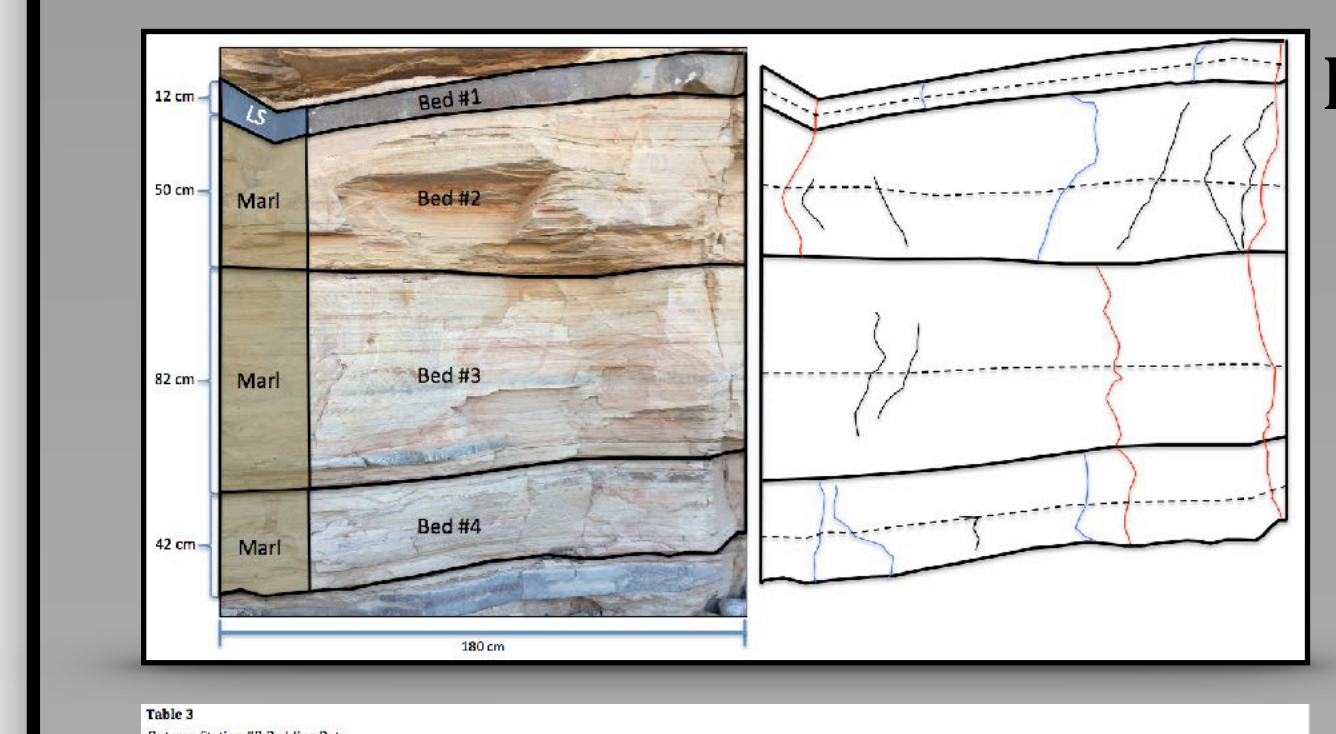


Figure 11 A-D: Stereonet data of bedding planes for outcrop stations 1-4 (A-D) respectively.

Table 3: Summary of Fracture Data for Station 3. Columns include Fracture ID, Orientation, Length, Frequency, etc.

Table 4: Summary of Fracture Data for Station 4. Columns include Fracture ID, Orientation, Length, Frequency, etc.

Table 5: Summary of Fracture Data for Station 1. Columns include Fracture ID, Orientation, Length, Frequency, etc.

Table 6: Summary of Fracture Data for Station 2. Columns include Fracture ID, Orientation, Length, Frequency, etc.

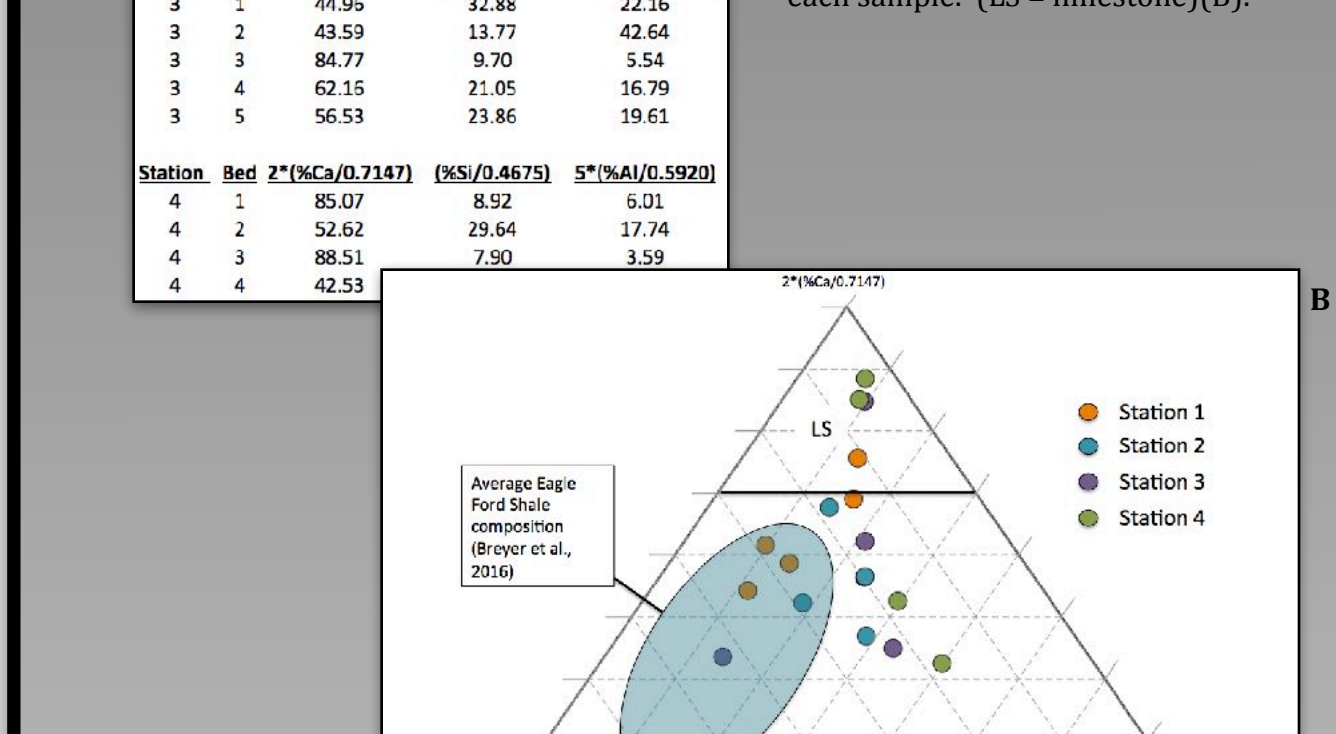


Figure 12 A-D: Stereonet data of fractures for outcrop stations 1-4 (A-D) respectively.

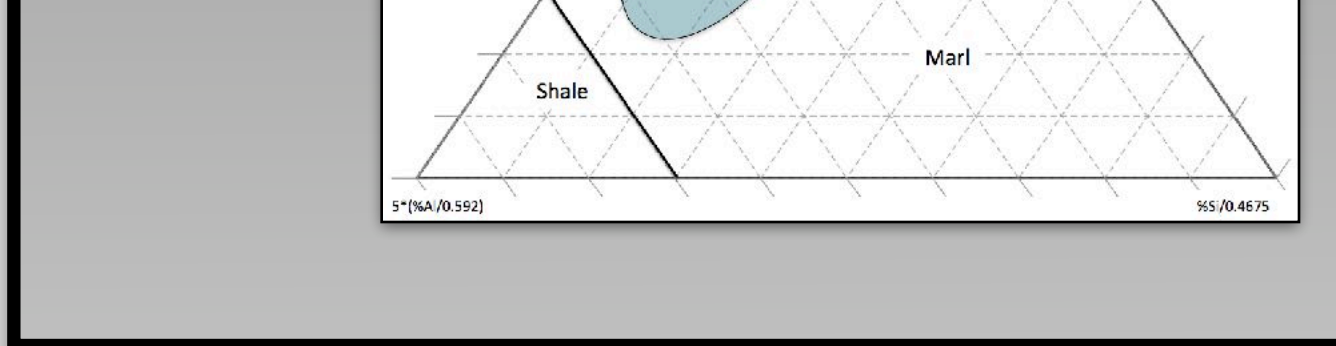


Figure 13 A & B: XRF data for all beds within each outcrop station. UCS vs calcite (%Ca) shows a positive correlation (A). UCS vs quartz (%Si) shows no trend (B), whereas UCS vs clay (%Al) shows a negative correlation (C).

Analysis

High angle normal faults associated with Tertiary Basin and Range extension are responsible for the present day topography within the mapping area. The deformation associated with Basin and Range extension caused the tilting of geologic units as well as forming half-graben structures along high-angle normal faults which juxtapose older and younger rocks (Fig. 15 A & B).

Fractures are more likely to be through-going in layers of more competent rock. Conversely, fractures were more likely to terminate within or at the contact of a bed in the thicker less competent rock (Figure 10 A-D).

In general, fractures within each outcrop can be divided into 2 sets: Set 1 average strike/dip is 223°/63°. Set 2 average strike/dip is 53°/55° (Figs. X A-D). Maximum paleostress directions can be inferred based on this conjugate set, roughly NE/SW in this case (Fig. 16).

Rocks of the Boquillas Formation tend to be more calcareous with certain layers containing higher clay and quartz content. Overall, the Boquillas Formation at this location is more clay-poor than the average Eagle Ford Shale composition (Figure 13 A & B).

Cross-plots of XRF vs. UCS suggest that strength of the rock increases as calcite content increase and clay content decreases. Additionally, the dimpler method showed a stronger correlation with elemental data than the Bambino. The Bambino requires a relatively smooth surface to take measurements on while the dimpler does not. This could be one reason for the difference in UCS values (14 A, B, & C).

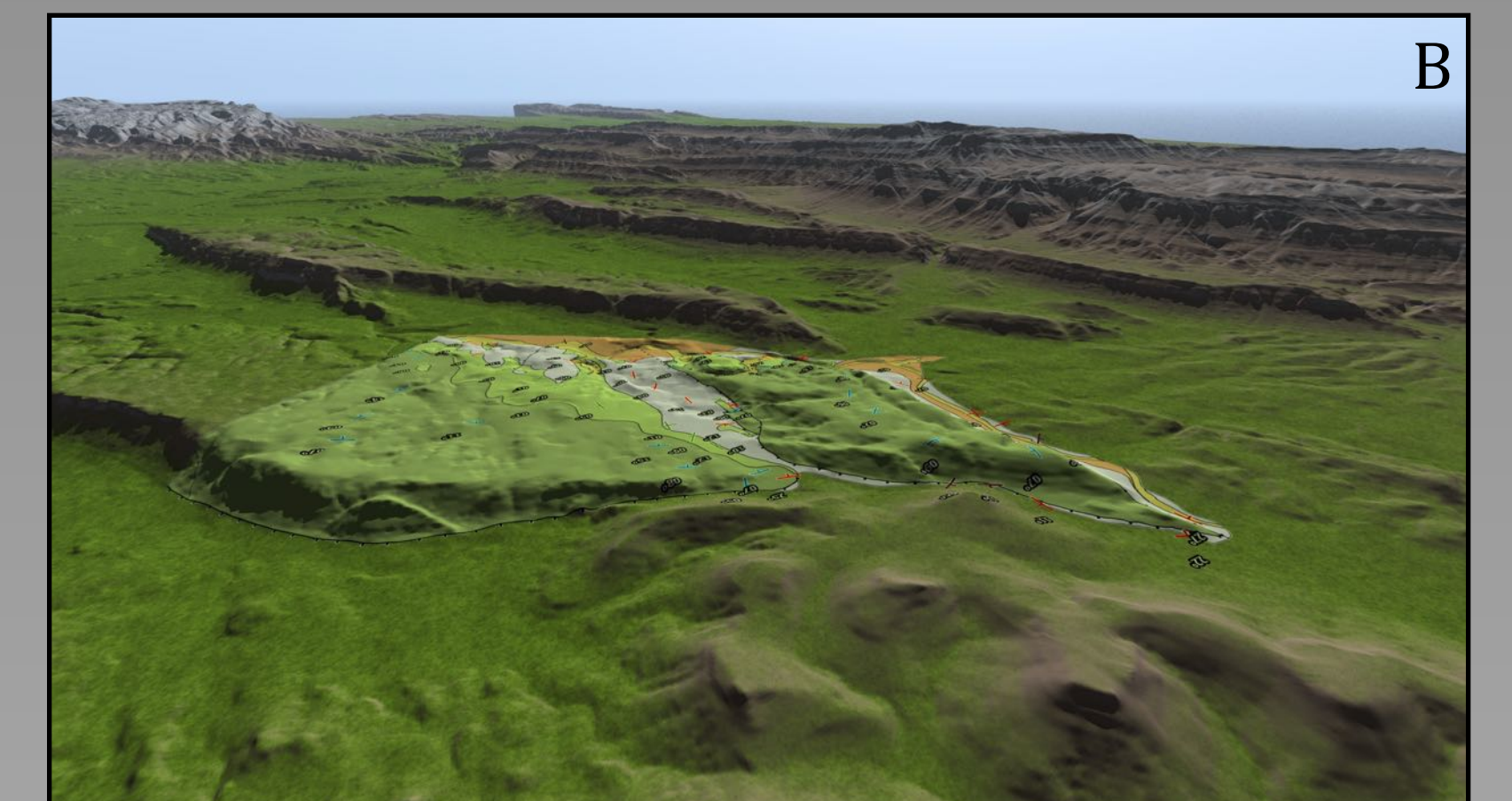


Figure 15 A & B: Geologic map drawn over a digital elevation model of Heath Canyon and the surrounding area. View looking south-southwest (A) and a view looking west-southwest (B).

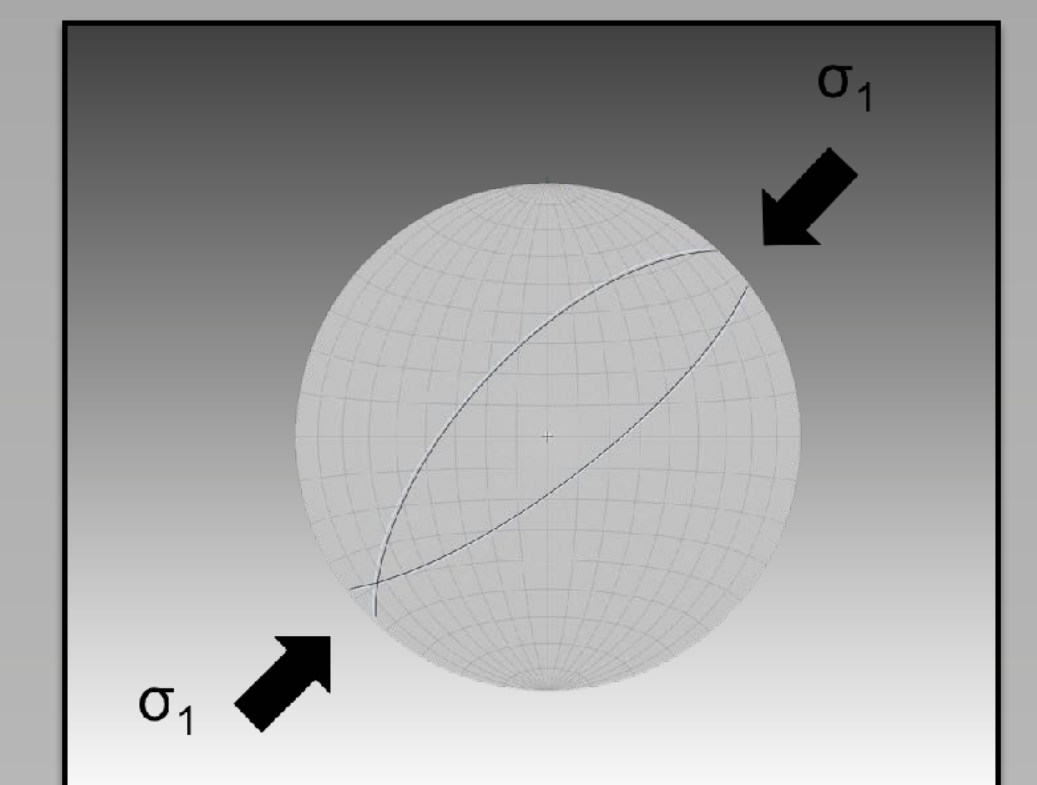


Figure 16: Stereonet displaying the orientation of both sets of fracture with inferred paleostress directions.

Conclusions

- Stratigraphic units along with prominent topographic features located near Heath Canyon may reflect the stresses of two major deformational episodes: Laramide-related shortening and Basin and Range extension. Shortening stresses during the Laramide Orogeny produced the Sierra del Carmen Mountains, the high peaks within along the western border of Black Gap WMA. The location of the study area may be a north-eastern extension of this mountain range. Basin and Range extensional stresses generated high-angle normal faults and half-graben structures which juxtapose Santa Elena Limestone against the younger Buda Limestone and Boquillas Formation. These faults are consistent with Basin and Range-related high-angle normal faults within Big Bend National Park. Additionally, as a result of this faulting, stratigraphic units within the area are tilted -10°-15° to the southwest.
- Fracture analysis of the Boquillas Formation within Heath Canyon reveals a conjugate set of fractures. Set 1 has an average strike/dip of 223°/63°. Set 2 has an average strike and dip of 53°/55°. Paleostress directions may be inferred as roughly northeast/southwest based on the average strike of these fracture sets which is consistent with the paleostress directions associated with Laramide deformation.
- Previous studies show a linear relationship between mode I fracture spacing and bed thickness. Data in this study show a non-linear trend between these two variables which suggests that the Boquillas Formation fractures differently than the formations analyzed in previous studies, the fractures seen in this study are not mode I fractures, or that the classification of layering for this study was incorrect.
- Lithology may play a role in the vertical persistence of fractures. XRF analysis allows the carbonate rock layers of the Boquillas Formation to be classified into either calcite dominant limestones or calcite-clay dominant marls. These two chemically distinct rock types exhibit differing rock strength values. Limestone layers generally have higher strength values than marl layers, a function of higher calcite and lower clay content. Due to the strength, limestones behave in a more brittle manner than marls allowing fractures to propagate more readily.
- Though previous studies suggest the nature of bed-to-bed transitions, gradational or abrupt, affect the vertical persistence of fractures, data produced in this study show little difference in the frequency of through-going fractures when the layer interface is gradational or abrupt within limestone-to-marl transitions. However, when the interface is composed of thin ash beds, there is a marked decrease in the frequency of through-going fractures.

References

Breyer, J.A. 2016. Introduction in AAPG Memoir 110: The Eagle Ford Shale: A renaissance in U.S. oil production, pp. 259-283.

Bruker 2015. Tracer series overview. Accessed: April 6, 2015. <https://www.bruker.com/products/x-ray-diffraction-and-elemental-analysis/handheld-xrf/tracer-iii-overview.html>

Lehman, T.M., and Busbey, A.B., 2007. Society of Vertebrate Paleontology Fall 2007 Big Bend Field Trip Guidebook, Austin, Society of Vertebrate Paleontology.

Muehlberger, W.R., and Dickerson, P.W., 1989. Structure and stratigraphy of Trans-Pecos Texas: El Paso to Guadalupe Mountains and Big Bend Guidebook, 20-29 July, Washington, D.C.: American Geophysical Union.

Maxwell, L.A., Lonsdale, J.T., Hazzard, R.T. and Wilson, J.A., 1967. Geology of Big Bend National Park, Brewster County, Texas. University of Texas at Austin, Bureau of Economic Geology, Texas Univ. Pub. 6711.

Proceq, Equotip Bambino 2 Proceq Metal Hardness Testers. Last modified October 17, 2016. <http://www.proceq.com/jp/nondestructivetesting/metal-testing/hardness-testing/equotip-bambino-2.html>

Railroad Commission of Texas (Texas RRC) 2016. Eagle Ford Shale Information. Last modified: April 5. Accessed April 13, 2016. <http://www.rrc.state.tx.us/oil-gas/major-oil-gas-formations/eagle-ford-shale/>

St. John, R. 1966. Geology of Black Gap Area, Brewster County, Texas. geological quadrangle map GQ-0030 Bureau of Economic Geology, vol. 18, University of Texas at Austin (1966) geologic map scale: 1:62,500

Tiedemann, N.S. 2010. The sequence stratigraphy of the Comanchean - Gulfian interval, Big Bend National Park, West Texas. [Master's thesis] Ball State University.

Turner, K.J., Berry, M.E., Page, W.R., Lehman, T.M., Bohannon, R.G., Scott, R.B., Miggins, D.P., Bodahn, J.R., Cooper, R.W., and Drenth, B.J., 2011. Geologic map of Big Bend National Park, Texas. US Department of the Interior, US Geological Survey.

U.S. Energy Information Administration (EIA) 2016. Drilling productivity report. Last modified September 12. Accessed October 25, 2016 <http://www.eia.gov/petroleum/drilling/archive/2016/09/>